Unique Photochemical Properties of p-Substituted Cationic Triphenylbenzene Derivatives on a Clay Layer Surface

ARTICLE *in* THE JOURNAL OF PHYSICAL CHEMISTRY C · JANUARY 2013

Impact Factor: 4.77 · DOI: 10.1021/jp3092144

3 AUTHORS, INCLUDING:

Shinsuke Takagi
Tokyo Metropolitan University
86 PUBLICATIONS **1,492** CITATIONS

THE JOURNAL OF PHYSICAL CHEMISTRY C

Article

pubs.acs.org/JPCC

Unique Photochemical Properties of *p*-Substituted Cationic Triphenylbenzene Derivatives on a Clay Layer Surface

Takamasa Tsukamoto,[†] Tetsuya Shimada,[†] and Shinsuke Takagi*[,†,‡]

[†]Department of Applied Chemistry, Graduate Course of Urban Environmental Sciences, Tokyo Metropolitan University, Minami-ohsawa 1-1, Hachiohji, Tokyo 192-0397, Japan

[‡]PRESTO (Precursory Research for Embryonic Science and Technology), Japan Science and Technology Agency, 4-1-8 Honcho Kawaguchi, Saitama, Japan

Supporting Information

ABSTRACT: Two types of novel tricationic 1,3,5-triphenylbenzene (TPB) derivatives were synthesized. The TPB derivatives are 1,3,5-tris(*N*,*N*,*N*-trimethylanilinium-4-yl)-benzene (TMAB) and 1,3,5-tris[(*N*-pyridinium)aniline-4-yl]-benzene (TPAB). The photochemical behaviors of both cationic TPBs with and without clay were examined in aqueous solution. For both TPBs, the aggregation behavior was not observed in the clay complexes even at saturated adsorption conditions. Interestingly, the fluorescence intensity of TPAB was extremely increased by the complex formation with clay compared to that without clay in a bulk aqueous solution, although the increase of fluorescence was not observed for TMAB. Time-resolved fluorescence measurement revealed that the increase of fluorescence turned out to be due to the suppression of the nonradiative deactivation process from its excited singlet state, because the molecular motion of TPAB should be restricted due to the strong fixation on the clay surface. TPAB exhibited a little self-fluorescence quenching behavior as the loadings increased, while TMAB exhibited obvious self-fluorescence quenching on the clay surface. The difference of adsorption strength of TPBs onto the clay surface is supposed to affect their photochemical properties such as the increase of fluorescence and the self-fluorescence quenching behavior in the excited singlet state. It was found that the pyridinium substituent as cationic sites is beneficial to construct efficient photochemical reaction systems using a clay complex without unexpected fluorescence quenching.

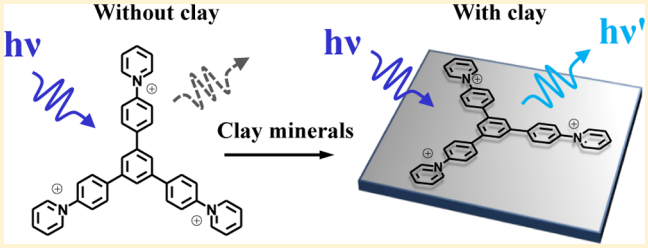

INTRODUCTION

Clay minerals[1−10] are well-known as multilayered inorganic materials that have quasi-two-dimensional spaces. Clay minerals have a cation exchange capacity (CEC) due to the negative charged face of nanosheets. The structure of typical clay (synthetic saponite) is shown in Figure 1. The stoichiometric formula is $[(Si_{7.2}Al_{0.8})(Mg_{5.97}Al_{0.03})O_{20}(OH)_4]^{-0.77}\cdot(Na_{0.49}Mg_{0.14})^{+0.77}$, the theoretical surface area is 750 $m^2\ g^{-1}$, and the cationic exchange capacity (CEC) is 0.997 mequiv g^{-1}.[11] The average area per anionic site is calculated to be 1.25 nm^2, and the average distance between anionic sites on the clay surface is estimated to be 1.2 nm, on the basis of the assumption of a hexagonal array.[11] Since the aqueous solution of saponite is transparent in the UV−visible range when the particle size is small (<200 nm),[11] they are suitable for constructing the photochemical reaction systems.[12]

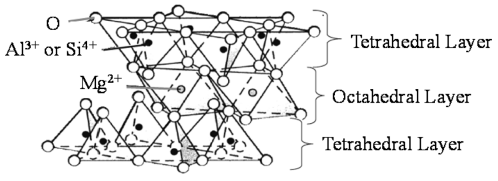

Figure 1. The structure of synthetic saponite, $[(Si_{7.2}Al_{0.8})(Mg_{5.97}Al_{0.03})O_{20}(OH)_4]^{-0.77}$.

The adsorption or intercalation of cationic organic molecules on or into the clay layer structure can afford very interesting inorganic−organic hybrid compounds. Adsorption properties of many different types of cationic dye molecules have been investigated.[2,7,8,14−26] Generally, the adsorbed molecules tend to be aggregated on or in the clay layer structure.[13] Since an aggregation such as H-aggregation in general decreases the excited-state lifetimes of dyes drastically, the formation of aggregates is not favored for photochemical reactions. The control of the aggregation behavior of dyes on the clay surface has been considered difficult, in the past. Recently, we reported that +4-charged porphyrin molecules adsorb on nanosheets of saponite without aggregation even at high dye loadings.[27−32]

The unique photochemical behaviors of the dyes in the clay complex have been reported. The absorption maxima of porphyrin are shifted to longer wavelength by the complex formation with clay.[22,23,32] These interesting observations were

Received: September 17, 2012
Revised: December 18, 2012
Published: January 17, 2013

   dx.doi.org/10.1021/jp3092144 | *J. Phys. Chem. C* 2013, 117, 2774−2779

rationalized by a size-matching of the distances between the cationic sites in porphyrin molecules and anionic sites on the clay surface. We named this effect the "size-matching rule".[11,30−32] Methylviologen clay complexes (MV/clay) were investigated in detail.[33,34] Methylviologen dichloride (1,1′-dimethyl-4,4′-dipyridinium dichloride), that is, +2-charged organic molecule, can be intercalated into clay nanosheet layers. While MV is not emissive in aqueous solution, MV emits strong fluorescence in the clay complex. This unique fluorescence behavior of MV would be rationalized by the decrease of nonradiative deactivation processes in motionless flat configuration, although the detail is still unknown.[33,34] The fluorescence of dye molecules tends to be quenched by the self-quenching process on the clay surface. This behavior is also not favored for the construction of efficient photochemical reaction systems. We reported that some "size-matching" porphyrins do not suffer self-fluorescence quenching even at 100% adsorption vs the CEC of the clay.[35,36]

Although "size-matching" cationic porphyrin derivatives were well investigated,[11,27−32,35,36] the adsorption behaviors of other dyes that fulfill the "size-matching rule" on the clay surface have not been examined well. In this work, we designed and synthesized the novel cationic molecules that are expected to fulfill the "size-matching rule" on the saponite surface. Two types of novel tricationic triphenylbenzene (TPB) derivatives were synthesized. The TPB derivatives are 1,3,5-tris(*N*,*N*,*N*-trimethylanilinium-4-yl)benzene (TMAB) and 1,3,5-tris[(*N*-pyridinium)aniline-4-yl]benzene (TPAB) (Figure 2). Both distances between adjacent cationic sites in TPB molecules were estimated to be about 1.25 nm, which is close to the average distance between anionic sites on the clay surface and fulfills the "size-matching rule". The adsorption behavior and photochemical properties of these cationic TPB derivatives on the anionic clay surface were investigated by UV−visible absorption, fluorescence spectra, and time-resolved fluorescence spectra by controlling the loading levels of cationic TPBs vs the CEC of the clay.

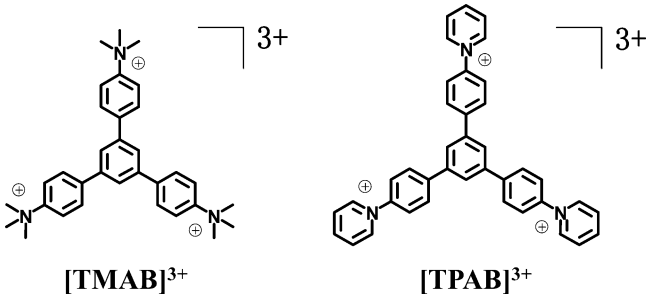

Figure 2. Structures of 1,3,5-tris(*N*,*N*,*N*-trimethylanilinium-4-yl)-benzene (TMAB) and 1,3,5-tris[(*N*-pyridinium)aniline-4-yl]benzene (TPAB).

EXPERIMENTAL SECTION

Materials and Measurement. Clay Minerals (saponite): Sumecton SA was received from Kunimine Industries Co., Ltd. 1,3,5-Tris(4-*N*,*N*,*N*-trimethylanilinium)benzene trichloride ([TMAB]Cl_3) and 1,3,5-tris[(*N*-pyridinium)aniline-4-yl]-benzene trichloride ([TPAB]Cl_3) were synthesized using a method described in the Supporting Information.

UV−visible absorption spectra were obtained on a Shimadzu UV-3150 spectrophotometer. Emission spectra were recorded on a Jasco FP-6600 spectrofluorometer. Time-resolved fluorescence signals were measured by a Hamamatsu Photonics C4780 system based on a streak detector. The fourth harmonic (266 nm) of an Nd^{3+} YAG laser (EKSPLA PL2143B, fwhm 25 ps, 5 Hz) was used for excitation.

DFT calculations were performed at the B3LYP/6-31G* level with the Gaussian 09 package.[37] In the optimized structure, the distances of *N* to *N* in TMAB and TPAB molecules are estimated to be 1.24 and 1.25 nm (Figure S3 in the Supporting Information).

Sample Preparation for Absorption Spectra. Exfoliated TPB−saponite complexes were prepared by mixing aqueous clay colloidal suspensions and the respective cationic TPB aqueous solutions under stirring. The concentration of clay for a Lambert−Beer plot was 4.0×10^{-6} equiv L^{-1}. The loading levels of cationic TPB vs the CEC of the clay in the complexes were controlled by varying the concentration of TPB.

Sample Preparation for Fluorescence Spectra. The preparation method for the TPB/saponite complex is the same as that for the absorption spectra. The concentration of TPB was 1.0×10^{-6} M. The loading levels of cationic TPB vs the CEC of the clay in the complexes were controlled by varying the concentration of clay.

Sample Preparation for Time-Resolved Fluorescence Spectra. The preparation method for the TPB/saponite

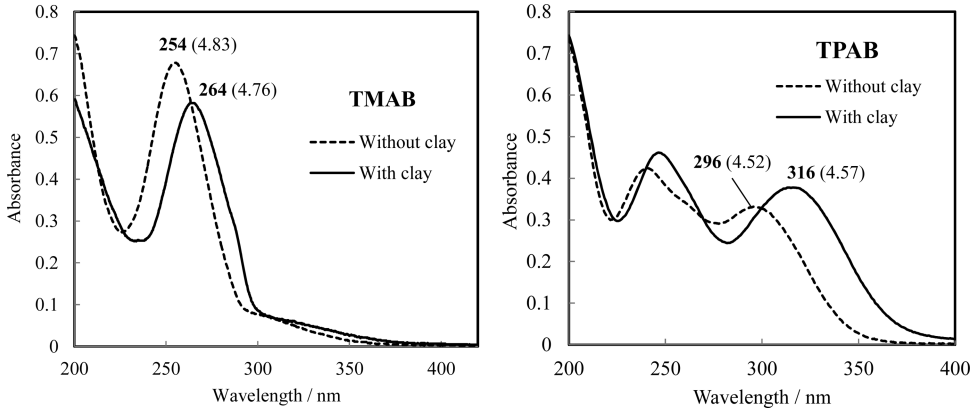

Figure 3. Absorption spectra and absorption maxima values (λ_{max}, nm) of the longest-wavelength peak of TMAB (left) and TPAB (right) with and without clay. The extinction coefficients ($\log \varepsilon_{max}$) are shown in the brackets. [TPB] = 1.0×10^{-5} M, [saponite] = 6.0×10^{-5} equiv L^{-1} (the loading levels of cationic TPBs are 50% vs the CEC of the clay).

dx.doi.org/10.1021/jp3092144 | J. Phys. Chem. C 2013, 117, 2774−2779

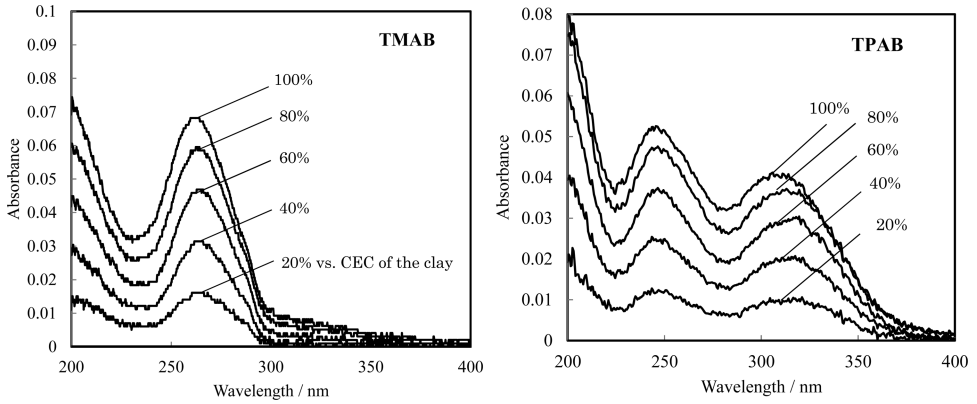

Figure 4. Absorption spectra of the TMAB/saponite complex (left) and the TPAB/saponite complex (right) at various TPB concentrations in aqueous transparent colloid solution, up to 100% vs CEC ([saponite] = 4.0×10^{-6} equiv L^{-1}).

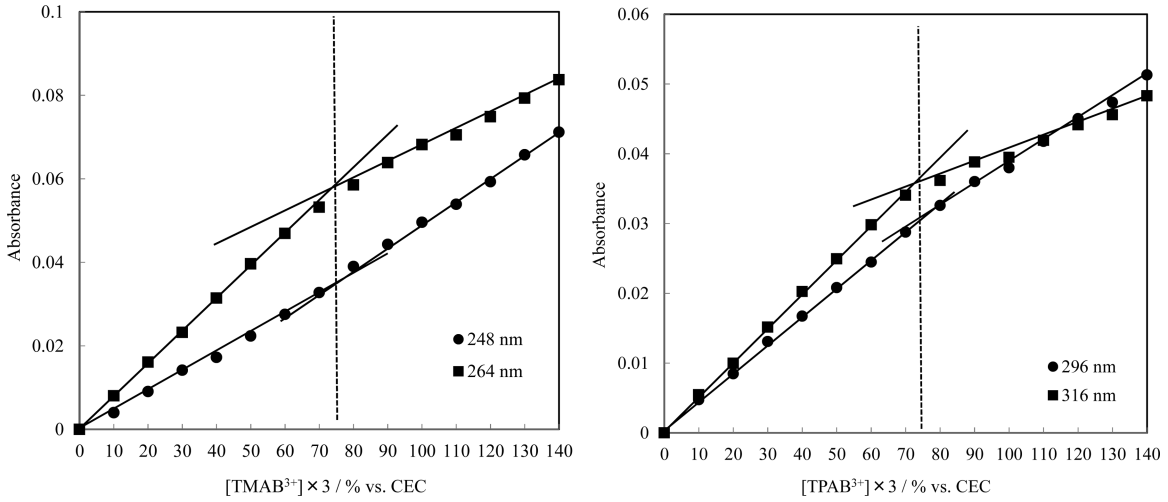

Figure 5. Lambert–Beer plots for the TMAB/saponite complex at 248 nm (●) and 264 nm (■) (left) and for the TPAB/saponite complex at 296 nm (●) and 316 nm (■) (right) in aqueous transparent colloidal solution.

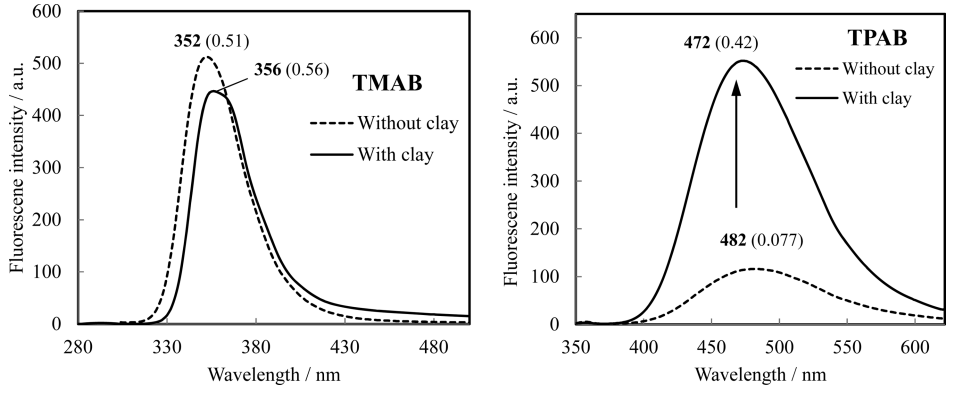

Figure 6. Fluorescence spectra and fluorescence peaks (λ_{em}, nm) of TMAB excited at 264 nm (left) and TPAB excited at 316 nm (right) with and without clay. The fluorescence quantum yields (Φ_f) are shown in the brackets. [TPB] = 1.0×10^{-6} M, [saponite] = 3.0×10^{-5} equiv L^{-1} (the loading level of TPB was 10% vs the CEC of the clay).

complex is the same as that for the absorption spectra. The concentration of TPB was 1.0×10^{-6} M. The TPB loadings are set at 9% vs the CEC of the clay.

■ RESULTS AND DISCUSSION

Absorption Spectra of TPBs with and without Clay. The aqueous clay colloidal suspension was essentially transparent in the UV–visible region under the present experimental conditions. UV–visible absorption spectra of the TPBs in water and adsorbed on the saponite surface were observed. The absorption spectra of TMAB and TPAB with and without clay are shown in Figure 3.

Author: Please double-check the wording for the following sentence.Both cationic TPBs, clay complexes exhibited the spectral shift to longer wavelengths, compared to those in the

dx.doi.org/10.1021/jp3092144 | J. Phys. Chem. C 2013, 117, 2774–2779

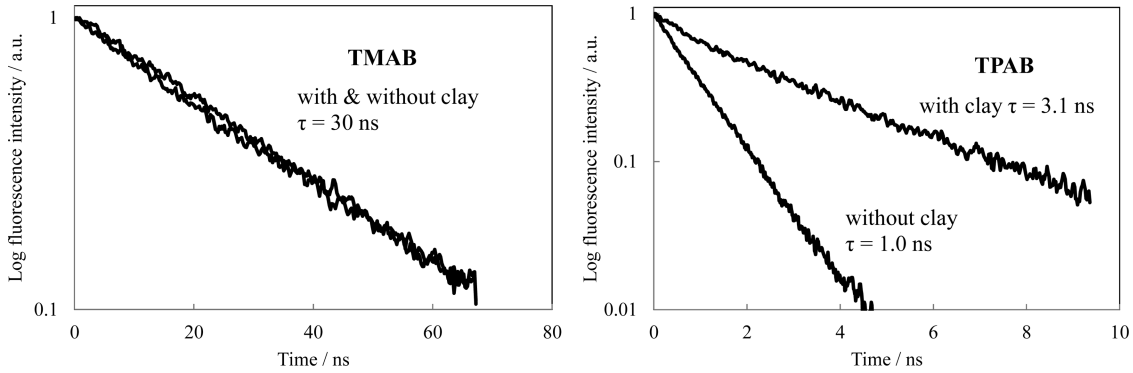

Figure 7. The fluorescence decay profiles and fluorescence lifetimes (τ) of TMAB (left) and TPAB (right) excited at 266 nm with and without clay. The fluorescence of TMAB and TPAB was monitored from 316 to 455 nm and from 415 to 550 nm, respectively. The loading levels of TPBs were 9% vs the CEC of the clay.

bulk solution. These red shifts would be induced by the molecular flattening of TPBs that extends the π conjugation in the molecule, upon adsorption on the clay surface.[38] Because the bulky trimethylammonium group of TMAB suppresses the molecular flattening, the degree of red shift in TMAB is smaller than that of TPAB. The maximum adsorption amounts of TPBs without aggregation were determined by measuring the absorption spectra at various dye loadings, as shown in Figure 4 (more detailed absorption spectra are shown in Figure S4 in the Supporting Information). The absorption spectra retained the same shape at 10−70% vs CEC for both TPBs. Above 70% adsorption, nonadsorbed TPBs in bulk solutions were newly superimposed on the spectra. The linearity of Lambert−Beer plots also indicates that the aggregation is completely suppressed (Figure 5). Judging from the Lambert−Beer plots, the maximum adsorption amounts of both TPBs were determined to be 75% vs CEC. The average distance between TPB molecules is estimated to be 2.4 nm (center to center). This distance is equal to that of tetra-cationic porphyrins adsorbed 100% vs CEC. These results indicate that the novel two types of TPBs almost fulfill the "size-matching rule" as we expected.

Fluorescence measurement of TPBs with and without Clay. Fluorescence spectra of the TPBs in water and adsorbed on the saponite surface were observed. The fluorescence spectra of TMAB and TPAB with and without clay are shown in Figure 6.

In the case of TMAB, a slight red shift (4 nm) of the fluorescence maximum (λ_{em}) was observed by the complex formation with clay. The fluorescence intensity of TMAB on the clay surface slightly decreased compared with that in water. In the case of TPAB, a blue shift (10 nm) of λ_{em} was observed by the complex formation with clay. The fluorescence intensity of TPAB on the clay surface extremely increased about 5 times as much as that in water. This blue shift of λ_{em} and the increase of fluorescence intensity on the clay surface are very interesting from the viewpoint of photochemistry. These observations would be rationalized by the decrease of nonradiative deactivation processes in the motionless flat configuration of TPAB on the clay surface.[33,34] In the case of TMAB, those behaviors were not observed because TMAB cannot be flattened well due to the steric hindrance of the ammonium substituent.

To discuss the detail of the photochemical behavior of TPBs on the clay surface, the time-resolved fluorescence spectra for each TPB/clay complex were measured to obtain the excited lifetime by using the picosecond fluorescence measurement system. As shown in Figure 7, both decay curves for TPB/clay complexes can be analyzed as a single exponential decay. In this experiment, the TPB loadings were set at 9% vs the CEC of the clay.

The radiative deactivation rate constant for fluorescence (k_f) and nonradiative deactivation rate constant (k_{nr}) were calculated from the fluorescence quantum yields (Φ_f) and fluorescence lifetime (τ) according to eqs 1 and 2, as shown in Table 1.

$$\Phi_f = \frac{k_f}{k_f + k_{nr}} \quad (1)$$

$$\tau = \frac{1}{k_f + k_{nr}} \quad (2)$$

Table 1. The Deactivation Rate Constants of TPBs in Water and on the Clay Surface

	k_f (ns^{-1})		k_{nr} (ns^{-1})	
compound	without clay	with clay	without clay	with clay
TMAB	0.017	0.015	0.016	0.018
TPAB	0.081	0.13	0.97	0.19

In the case of TMAB, the k_f and k_{nr} values were not affected by the complex formation with clay. On the other hand, in the case of TPAB on the clay surface, k_f was increased and k_{nr} was drastically decreased compared to those without clay. These results can be qualitatively rationalized as follows. Considering the Franck−Condon principle, these behaviors could be discussed by the use of potential curves of the ground and excited state of TPAB with and without clay. The potential energy curve of TPBs must be affected by the complex formation with clay. With clay, it is expected that (i) the most stable structure is relatively similar between the ground and excited states (effect i) and (ii) the potential energy curve is relatively sensitive against the nuclear coordinates (effect ii), compared to those without clay. Thus, the potential curve of TPAB with and without clay can be qualitatively illustrated as shown in Figure 8. In the case of potential energy curves with clay, the larger Franck−Condon factor seems to rationalize the larger k_f value compared to those without clay. In the same manner, it is expected that the Franck−Condon factor for k_{nr} would be smaller for the clay complex, since the potential

dx.doi.org/10.1021/jp3092144 | J. Phys. Chem. C 2013, 117, 2774−2779

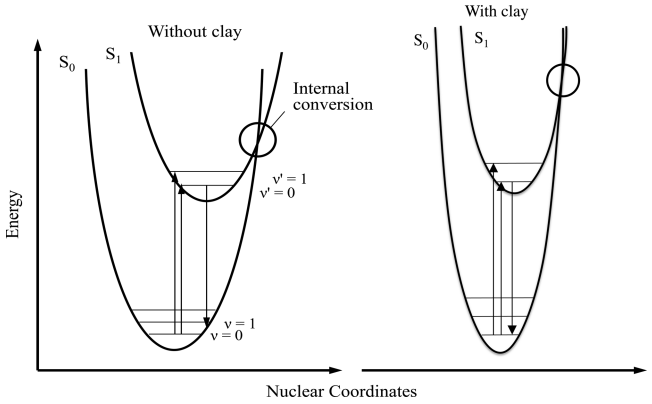

Figure 8. Plausible potential energy curves of the ground and excited states of TPAB with and without clay.

energy curves for the ground and excited states cross at the high vibration state of the excited state's potential energy curve. In other words, since the structure of TPAB is fixed and the vibrational mobility is suppressed on the clay surface, k_{nr} was drastically decreased by the complex formation with clay.

Self-Fluorescence Quenching Behavior of TPBs with and without Clay. The self-fluorescence quenching behavior of the TPB/clay complexes was examined. In the present system, the aggregation is completely suppressed and the decomposition due to UV−visible light irradiation was not detected in absorption spectra. Thus, the self-fluorescence quenching in this system is supposed to be induced by an electron transfer reaction between adjacent adsorbed molecules on the clay surface.[32,35] Fluorescence spectra of complexes for TMAB and TPAB at different loading levels are shown in Figure 9 (more detailed fluorescence spectra are shown in Figure S5 in the Supporting Information), respectively. The concentration of TPB was kept constant at 1.0×10^{-6} M to retain the same absorbance in all cases, and the loading level was changed by changing the concentration of clay. Thus, we can discuss the self-fluorescence quenching by simple comparison of the fluorescence intensity.

The pronounced fluorescence quenching and the increase of the broad spectral peak at around 480 nm, which is probably excimer emission, were observed for TMAB. Above 70% vs CEC adsorption, the fluorescence due to nonadsorbed TMAB in a bulk solution was newly superimposed on the spectra (not shown). On the other hand, fluorescence quenching was moderately observed up to 70% vs CEC for TPAB. Although TMAB and TPAB have the same number of cationic valence, in which the intracharge distances are almost same, the certain difference of self-fluorescence quenching behavior was observed. This can be rationalized by the difference of cationic substituents as described below. Judging from the red shifts in absorption spectra, both TPBs are forced to form a flat structure on the clay surface.[32] However, the difference of steric effects in cationic substituents on TPBs should be considered, as shown in Figure 10. TPAB having pyridinium substituents is able to approach the clay surface well due to the rotation of the pyridinium substituent. On the other hand, TMAB having trimethylammonium substituents is not able to approach enough due to the steric hindrance of ammonium substitutents.

A decrease of the distance between the cationic site of TPB and the clay surface increases the Coulomb's force between TPB and clay. Therefore, the adsorption strength of TMAB onto the clay surface should be weaker than that of TPAB. The weak adsorption should enhance the mobility and collision frequency of molecules, which is essentially needed for an electron transfer reaction. As a result, the fluorescence quenching of TMAB is larger than that of TPAB. Like this, two types of TPBs have interesting properties on the fluorescence behavior due to the difference of the molecular structure on the clay surface.

CONCLUSION

Two types of novel cationic TPB derivatives were synthesized successfully. The photochemical properties of both TPBs with and without clay were investigated. For both TPBs, aggregation behavior was not observed in the clay complexes even at saturated adsorption conditions, in accordance with the "size-matching rule" which was proposed recently by our group. The absorption spectra of TPB/clay complexes shifted to longer wavelength due to the flattening of the molecule on the clay surface. The red shift of TPAB complex (20 nm) was larger than that of TMAB complex (10 nm), because the TMAB cannot be flattened well due to the steric hindrance of the ammonium substituent. The maximum adsorption amounts of TMAB and TPAB on the clay surface were the same at about 75% vs the CEC of the clay, judging from the Lambert−Beer plots. However, the fluorescence properties of TPBs on the clay surface were different. The fluorescence intensity of the TPAB complex was drastically increased compared to that in water, while the increase of fluorescence intensity was not observed in

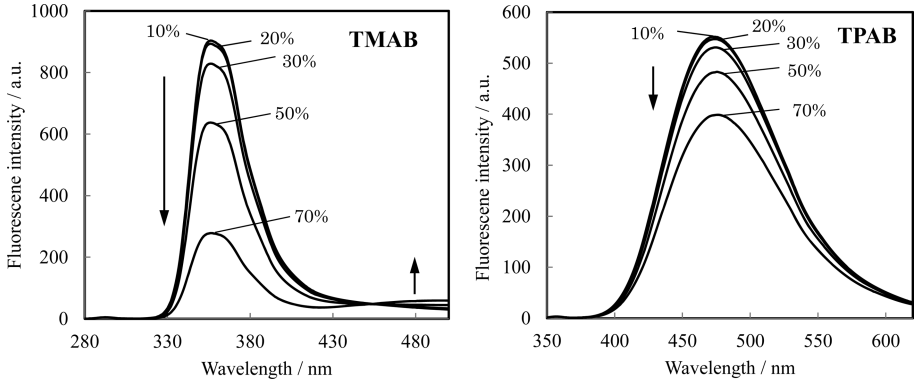

Figure 9. Fluorescence spectra of the TMAB/saponite complex excited at 264 nm (left) and the TPAB/saponite complex excited at 316 nm (right) with and without clay. [TPB] = 1×10^{-6} M.

dx.doi.org/10.1021/jp3092144 | J. Phys. Chem. C 2013, 117, 2774−2779

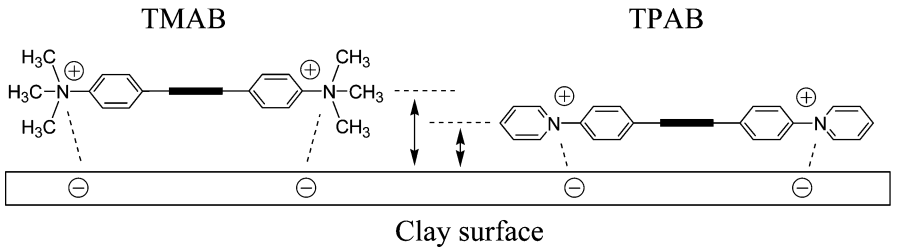

Figure 10. The schematic representation for the difference of distances between the cationic site of TPBs and the anionic site of clay.

the case of TMAB. Moreover, the fluorescence quenching of TPAB was less effective than that of TMAB. These unique fluorescence behaviors would be rationalized by the molecular structure of TPBs due to the difference of the host−guest interaction. These results indicate that the pyridinium substituent of cationic molecules is important to construct efficient photochemical reaction systems using a clay complex without unexpected fluorescence quenching. These findings are beneficial to expect the photochemical property of dyes and construct the efficient photochemical reaction systems in the dye−clay complexes.

■ ASSOCIATED CONTENT

Supporting Information

The synthesis procedure of TPBs, the ^{1}H NMR spectra of TMAB (Figure S1) and TPAB (Figure S2), the optimized structures of TPBs by DFT calculation (Figure S3), more detailed absorption spectra than Figure 4 (Figure S4), and more detailed fluorescence spectra than Figure 9 (Figure S5). This material is available free of charge via the Internet at http://pubs.acs.org.

■ AUTHOR INFORMATION

Corresponding Author

*E-mail: takagi-shinsuke@tmu.ac.jp. Phone: +81 42 677 2839. Fax: +81 42 677 2838.

Notes

The authors declare no competing financial interest.

■ ACKNOWLEDGMENTS

This work has been partly supported by a Grant-in-Aid for Precursory Research for Embryonic Science and Technology (PRESTO) from the Japan Science and Technology Agency (JST).

■ REFERENCES

(1) Kuroda, T.; Fujii, K.; Sakoda, K. *J. Phys. Chem. C* **2010**, *114*, 983−989.
(2) Okada, T.; Ide, Y.; Ogawa, M. *Chem.—Asian J.* **2012**, *7*, 1980−1992.
(3) Lopez Arbeloa, F.; Martinez, V.; Arbeloa, T.; Lopez Arbeloa, I. *J. Photochem. Photobiol., C* **2007**, *8*, 85−108.
(4) Ras, R.; Umemura, Y.; Johnston, C.; Yamagishi, A.; Schoonheydt, R. *Phys. Chem. Chem. Phys.* **2007**, *9*, 918−932.
(5) Sato, H.; Hiroe, Y.; Tamura, K.; Yamagishi, A. *J. Phys. Chem. B* **2005**, *109*, 18935−18941.
(6) Letaief, S.; Detellier, C. *Langmuir* **2009**, *25*, 10975−10979.
(7) Takagi, K.; Shichi, T. *J. Photochem. Photobiol., C* **2000**, *1*, 113−130.
(8) Takagi, S.; Eguchi, M.; Tryk, D, A.; Inoue, H. *J. Photochem. Photobiol., C* **2006**, *7*, 104−126.
(9) Thomas, J. K. *Chem. Rev.* **1993**, *93*, 301−320.
(10) Bujdak, J. *Appl. Clay Sci.* **2006**, *34*, 58−73.
(11) Takagi, S.; Shimada, T.; Eguchi, M.; Yui, T.; Yoshida, H.; Tryk, D. A.; Inoue, H. *Langmuir* **2002**, *18*, 2265−2272.
(12) Bujdak, J.; Komadel, P. *J. Phys. Chem. B* **1997**, *101*, 9065−9068.
(13) Yui, T.; Kobayashi, Y.; Yamada, Y.; Yano, K.; Fukushima, Y.; Torimoto, T.; Takagi, K. *ACS Appl. Mater. Interfaces* **2011**, *3*, 931−935.
(14) Thomas, K. J.; Sunoj, R. B.; Chandrasekhar, J.; Ramamurthy, V. *Langmuir* **2000**, *16*, 4912−4921.
(15) Inagaki, S.; Ohtani, O.; Goto, Y.; Okamoto, K.; Ikai, M.; Yamanaka, K.; Tani, T.; Okada, T. *Angew. Chem., Int. Ed.* **2009**, *48*, 4042−4046.
(16) Fujii, K.; Iyi, N.; Hashizume, H.; Shimomura, S.; Ando, T. *Chem. Mater.* **2009**, *21*, 1179−1181.
(17) Pushpito, G. K.; Bard, A. *J. Phys. Chem.* **1984**, *88*, 5519−5526.
(18) Grauer, Z.; Avnir, D.; Yariv, S. *Can. J. Chem.* **1984**, *62*, 1889−1894.
(19) Miyamoto, N.; Kawai, R.; Kuroda, K.; Ogawa, M. *Appl. Clay Sci.* **2000**, *16*, 161−170.
(20) Bujdak, J.; Iyi, N. *Clays Clay Miner.* **2002**, *50*, 446−454.
(21) Iyi, N.; Sasai, R.; Fujita, T.; Deguchi, T.; Sota, T.; Lopez Arbeloa, F.; Kitamura, K. *Appl. Clay Sci.* **2002**, *22*, 125−136.
(22) Chernia, Z.; Gill, D. *Langmuir* **1999**, *15*, 1625−1633.
(23) Kuykendall, V. G.; Thomas, J. K. *Langmuir* **1990**, *6*, 1350−1356.
(24) Kosiur, D. R. *Clays Clay Miner.* **1977**, *25*, 365−371.
(25) Cady, S. S.; Pinnavaia, T. J. *Inorg. Chem.* **1978**, *17*, 1501−1507.
(26) Dias, P. M.; Faria, D. L. A.; Constantino, V. R. L. *Clays Clay Miner.* **2005**, *53*, 361−371.
(27) Takagi, S.; Shimada, T.; Yui, T.; Inoue, H. *Chem. Lett.* **2001**, *30*, 128−129.
(28) Takagi, S.; Tryk, D. A.; Inoue, H. *J. Phys. Chem. B* **2002**, *106*, 5455.
(29) Takagi, S.; Eguchi, M.; Inoue, H. *Langmuir* **2006**, *22*, 406.
(30) Eguchi, M.; Takagi, S.; Tachibana, H.; Inoue, H. *J. Phys. Chem. Solids* **2004**, *65*, 403−407.
(31) Egawa, T.; Watanabe, H.; Fujimura, T.; Ishida, Y.; Yamato, M.; Masui, D.; Shimada, T.; Tachibana, H.; Inoue, H.; Takagi, S. *Langmuir* **2011**, *27*, 10722−10729.
(32) Ishida, Y.; Masui, D.; Shimada, T.; Tachibana, H.; Inoue, H.; Takagi, S. *J. Phys. Chem. C* **2011**, *116*, 7879−7885.
(33) Villemure, G.; Detellier, C.; Szabo, A. G. *J. Am. Chem. Soc.* **1986**, *108*, 4658−4659.
(34) Villemure, G.; Detellier, C.; Szabo, A. G. *Langmuir* **1991**, *7*, 1215−1221.
(35) Takagi, S.; Aratake, Y.; Konno, S.; Masui, D.; Shimada, T.; Tachibana, H.; Inoue, H. *Microporous Mesoporous Mater.* **2011**, *141*, 38−42.
(36) Ishida, Y.; Fujimura, T.; Masui, D.; Shimada, T.; Tachibana, H.; Inoue, H.; Takagi, S. *Clay Sci.* **2012**, *15*, 69−174.
(37) Frisch, M. J.; et al. *Gaussian 09*, revision A.1; Gaussian, Inc.: Wallingford, CT, 2009.
(38) Ishida, Y.; Masui, D.; Shimada, T.; Tachibana, H.; Inoue, H.; Takagi, S. *J. Phys. Chem. C* **2012**, *116*, 7879−7885.